American Mineralogist, Volume 82, pages 900–912, 1997

Marcasite oxidation in low-temperature acidic (pH 3.0) solutions: Mechanism and rate laws

M.J. Rinker, H.W. Nesbitt, and A.R. Pratt

Department of Earth Sciences, University of Western Ontario, London, Ontario N6A 5B7, Canada

Abstract

Marcasite surfaces were analyzed using X-ray photoelectron spectroscopy (XPS) and auger electron spectroscopy (AES). XPS data of a pristine marcasite surface are used as a template to examine the characteristics of a marcasite surface after exposure to vigorous cleaning procedures and after reaction in oxygenated and mildly acidic (pH 3.0) solution.

Minor changes are observed to the Fe($2p_{3/2}$) spectrum after cleaning the surface with concentrated HCl. A new species is observed at approximately 709 eV, representing 10–15% of the total Fe spectrum. Chloride was detected by XPS broadscans and OH^- was observed in the O(1s) spectrum. The new Fe species at 709 eV may be associated with either OH^- or Cl^-.

XPS sulfur spectrum of the surface exposed to oxygenated, HCl solution (pH = 3.0) indicates that polysulfide increases at the expense of disulfide. The Fe species observed at 709 eV is also present and represents 10–15% total Fe. XPS broadscan analyses indicate trace amounts of chloride. Oxide O^{2-} is absent from the O(1s) spectrum but OH^- is present. AES depth profiles reveal no compositionally distinct zones after reaction.

Leach rates for the aqueous oxidation of marcasite were determined at 25 °C in O-saturated chloride solution at pH 3.0. Two rate experiments were performed on crushed and sieved size fractions of marcasite: one sample was vigorously cleaned to investigate fundamental aspects of marcasite leaching and the other was untreated to simulate conditions found in natural environments. The oxidative leach rate of Fe(aq) from pristine marcasite is 4.25×10^{-5} mmol/(m^2·s). Analyses of aqueous S speciation reveal fluctuations in S content of oxidation state lower than SO_4^{2-}. The XPS results suggest that the fluctuation may result from periodic release of polysulfide to solution, after accumulation on the reactive marcasite surface.

Introduction

Marcasite is a naturally occurring phase of the Fe-S system, has an FeS_2 composition, and is a dimorph of pyrite. Marcasite forms at low temperatures (Newhouse 1925) and is often found as an alteration product of pyrrhotite oxidation in mine waste dumps (Fleet 1970; Jambor 1994; Pratt 1995). Oxidation of marcasite contributes toward the formation of acid mine drainage, the formation of acid sulfate soils, and the formation of sandstone-type U deposits (Wiersma and Rimstidt 1984).

The oxidation of marcasite contributes to acid generation according to the following overall reactions:

$$FeS_2 + 7/2O_2 + H_2O \rightarrow Fe^{2+} + 2SO_4^{2-} + 2H^+ \quad (1)$$

with O_2 as the oxidant (Garrels and Thompson 1960), and

$$FeS_2 + 14Fe^{3+} + 8H_2O \rightarrow 15Fe^{2+} + 2SO_4^{2-} + 16\ H^+ \quad (2)$$

with Fe^{3+} as the oxidant (Singer and Stumm 1970). Solution Fe^{2+} in the above reactions may be oxidized to Fe^{3+}, and therefore recycled as an oxidant according to:

$$Fe^{2+} + 1/4O_2(aq) + H^+ \rightarrow Fe^{3+} + 1/2H_2O \quad (3)$$

(Brown and Jurinak 1989). Oxidation of the S component of marcasite to sulfate requires a transfer of 14 electrons. Because only one or two electrons are transferred per elementary oxidation reaction (Nordstrom 1982), the complete oxidation of marcasite must be composed of several intermediate steps that cause the production of intermediate S products such as thiosulfate, sulfite (Moses et al. 1987), and possibly polysulfides. Here polysulfides include hydropolysulfides (or sulfanes) (Tossell et al. 1981) because they cannot be distinguished by X-ray photoelectron spectroscopy (XPS).

Investigations of sulfide oxidation are often achieved by grinding samples to a grain size representative of mine waste tailings. Typically samples are placed in a batch-type reaction vessel (Williamson and Rimstidt 1994), and analyses of aqueous Fe and S species are used to obtain information regarding the rate law for mineral oxidative dissolution. Attempts were made to use this type of analysis to propose a mechanism for oxidation (Lowson 1982; McKibben and Barnes 1986). Activation energies presented for the oxidative dissolution of marcasite and pyrite (Wiersma and Rimstidt 1984; McKibben and

0003–004X/97/0910–0900$05.00

Barnes 1986) suggest that oxidative dissolution is controlled by a surface reaction. A study of the near surface of sulfides by XPS and by Auger electron spectroscopy (AES) is, therefore, required to complete the investigation of the mechanism of oxidation.

Grinding samples in preparation for leaching may cause surface defects and oxidation products on the surface of the sample under investigation (Sasaki 1994). These defects and oxidation products must be removed from the sample surface by a vigorous cleaning procedure before Fe or S aqueous species can be used as reliable reaction progress variables. Moses et al. (1987) examined pyrite oxidation by Fe^{3+} and by dissolved O and also presented comparisons of pretreatment procedures. Their results suggest that boiling pyrite grains in concentrated HCl is an effective measure to remove the surface residue created during grinding and storage.

In the present work, the near surface of a pristine, vacuum-fractured marcasite surface is analyzed by XPS. The XPS results of the pristine surface are used as a template to examine the near surface of marcasite cleaned by boiling in concentrated HCl (Moses et al. 1987). A third marcasite sample was placed in an oxygenated and mildly acidic (pH 3.0) HCl solution for 6 h. The mechanism of oxidative dissolution of marcasite is discussed on the basis of the results of XPS and AES spectroscopy. This paper also reports experiments conducted to determine a rate law for the oxidation of marcasite by dissolved O in acidic low-temperature solutions. There are many ways to perform rate measurements and to analyze the data produced by these measurements. If the goal is to explain processes that occur during weathering of mine wastes, then sample preparation must be designed to produce materials with properties, including surface properties, similar to those produced during mineral processing. If however fundamental aspects of leaching are to be investigated, different preparations should be used. Both aspects are investigated here. Fe and S were monitored in experimental solutions because the concentration of Fe in solution is easily measured and a comparison of Fe and S data provide insight into reaction stoichiometry.

Experimental method

The marcasite examined in this study was a research grade marcasite specimen from Vintirov, Bohemia, Czech Republic. It was purchased from Wards Scientific Supplies, St. Catherines, Ontario, Canada. A portion of the sample was studied in polished section under reflected light microscopy. Crystallographic properties were investigated by X-ray diffraction methods on Rigaku diffractometers using Cu$K\alpha$ and Co$K\alpha$ radiation. Diffractograms were corrected to the SiO_2 101 peak (3.342 Å). Mineral composition was determined by repeated electron microprobe analysis using a Jeol JX A-8600 superprobe. Trace element analyses were obtained by X-ray fluorescence (XRF) using a Philips PW-1450 sequential wavelength dispersion spectrometer.

Surface analyses

Sample preparation. Mineral fragments were prepared following the procedure of Pratt et al. (1994a). Marcasite laths ($2 \times 2 \times 8$ mm) were cut with a water-cooled diamond saw, cleaned by rinsing with methanol for 2 min then dried in an argon gas-filled glove box. Marcasite laths were fractured in an inert atmosphere (XPS analytical chamber or argon-filled glove box), perpendicular to the growth *c* axis (fracture surface is the *a-b* plane), to expose a fresh surface. All further sample manipulation was also carried out within inert atmospheres (nitrogen gas or argon gas).

A single unreacted marcasite lath, fractured in the XPS analytical chamber under high vacuum (1×10^{-9} torr), was analyzed. The Fe(2p) and S(2p) XPS spectra of this vacuum-fractured specimen were used as a template against which to evaluate the effects of cleaning the sulfide surface in concentrated HCl and the effects of reaction with oxygenated acidic solutions.

A second marcasite lath, fractured in the argon-filled glove box, was placed in boiling concentrated HCl for 15 min. The lath was subsequently removed from solution and transferred to the XPS laboratory. The fractured surface, on which all analyses were conducted, was readily distinguished from the cut surfaces. The purpose was to investigate the near surface of marcasite after it is cleaned according to method three of Moses et al. (1987), a method designed to remove the oxidation products and structural defects created during grinding.

A third marcasite lath, also fractured in the argon-filled glove box, was placed immediately in 500 mL of solution previously adjusted to pH 3.0 by addition of research grade HCl. The solution was stirred by a top-mounted impeller that did not suspend the crystal yet created a vortex that kept the solution saturated with O_2. Reaction time was 6 h. The marcasite lath was transferred to the XPS laboratory. Afterward, the XPS samples were transferred to the AES laboratory for analyses.

Analytical instrumentation. XPS spectra were obtained using a Surface Science Laboratories SSX-100 X-ray photoelectron spectrometer with a monochromatized Al$K\alpha$ X-ray (1487 eV) source. The instrument is described by Chaney (1987). The base pressure in the analytical chamber was approximately 5×10^{-9} torr. The instrument work function was set to give a value of 84.00 eV for the Au($4f_{7/2}$) line of gold metal. The spectrometer was calibrated to give an energy difference of 875.5 ± 0.1 eV between Cu($2p_{3/2}$) and Cu(3p) lines.

XPS broadscans were acquired using an analyzer pass energy of 160 eV and an X-ray spot size of 600 μm. Narrow region XPS spectra were obtained using an analyzer pass energy of 25 eV and an X-ray spot size of 300 μm. XPS broadscan analyses of the near-surface of both reacted and unreacted marcasite samples were obtained using peak areas and theoretical cross sections from Scofield (1976). Scofield cross sections provide precise measurements but have limitations to accuracy (Nesbitt and

TABLE 1. XPS reference binding energies for surface chemical species

Species	Binding energy	Source
$Fe(2p_{3/2})$		
Fe^{2+}-S	707.00	Buckley and Woods (1987)
	707.00	Mycroft et al. (1990)
	707.00	Nesbitt and Muir (1994)
Fe^{3+}-S	708.75	Nesbitt and Muir (1994)
Fe^{3+}-O-OH	710.30	Nesbitt and Muir (1994)
S(2p)		
S_2^{2-}	162.3	Buckley and Woods (1985)
	162.5	Mycroft et al. (1990)
	162.40	Nesbitt and Muir (1994)
S^{2-}	161.65	Nesbitt and Muir (1994)
	161.25	Pratt et al. (1994a)
S_n^{2-}	163.7	Hyland and Bancroft (1989)
	163.3–163.7	Mycroft et al. (1990)
	163.60	Nesbitt and Muir (1994)
S^*SO_3	161.7	Moulder et al. (1992)
SS^*O_3	167.7	Moulder et al. (1992)
SO_3^{2-}	167.7	Moulder et al. (1992)
SO_4^{2-}	168.5	Jones et al. (1992)
O(1s)		
Hydroxide	531.4	McIntyre and Zetaruk (1977)
	531.4	Mills and Sullivan (1983)
Chemically attached H_2O	532.4	Nesbitt and Muir (1994)
Physically adsorbed O_2	532.5	McIntyre and Zetaruk (1977)
Adsorbed H_2O	533.5	Knipe et al. (1995)
	533.5	Knipe et al. (1995)

Note: All values are reported in eV.

Muir 1994; McIntyre et al. 1996). Reliable interpretations can, however, be obtained by analyses of ion ratios rather than quantitative analyses (Pratt et al. 1994a). Narrow scans of the O(1s), $Fe(2p_{3/2})$, and $S(2p_{3/2})$ were collected to determine chemical state information using a true Shirley background (Shirley 1972) and a 70% Gaussian-30% Lorentzian peak model (Nesbitt and Muir 1994; Pratt et al. 1994a). XPS reference binding energies for chemical species considered here are listed in Table 1. Errors quoted for surface species throughout the text were obtained by varying the fit parameters of all species contributing to the spectrum and noting the extremes in species abundances. Averages of these extremes are quoted in Table 1 and percentage errors on species abundances are derived from the extreme in abundances. Additional details are given in Nesbitt and Muir (1994).

AES spectra were obtained using a Perkin-Elmer Phi 600 scanning Auger microprobe equipped with a secondary electron detector and an Ar^+ ion gun. Analyses were obtained using an electron beam accelerated to a potential of 3.0 kV at a current of 10 nA. Survey and depth profiles were obtained by rastering a nearly 30° incident 2.0 kV Ar^+ beam focused to a 2×2 mm spot size (Pratt et al. 1994b). A sputter rate of 30 Å/min was chosen on the basis of density similarities of marcasite to arsenopyrite (Nesbitt et al. 1995).

Aqueous analyses

Sample preparation. Samples prepared for analysis were crushed from coarse-grained massive specimens using a quartz mortar and pestle, then dry sieved to isolate the fraction of grains with diameters in the range of 125 to 250 μm. One portion of the crushed sample was added to 50 mL of concentrated (65%) HCl and boiled for 15 min. The samples were removed and rinsed with alternating baths of concentrated HCl and acetone then immediately transferred to an argon gas-filled glove box. The remaining portion of crushed sample was stored directly in the argonfilled glove box without pre-treatment. A sample weighing 1.00 ± 0.01 g was used in each experiment.

Surface areas were calculated assuming that grains were spherical and that each 1 g sample within the 125 to 250 μm diameter range had the same grain size distribution (Gaussian), with an average diameter of 187.5 μm. From these assumptions the total marcasite surface area was calculated to be 0.0064 m^2/g. Calculations obtained from total dissolved Fe, surface area, and unit cell size suggest that less than 0.1% of the total surface area reacts during the course of the experiment. Therefore, the average surface area calculated before the experiment is also considered to be the surface area during and after reaction. This value is used to normalize rates to 1 m^2 surface area.

Solutions. Solutions of pH 3.0 were prepared by combining concentrated HCl with de-ionized water that was obtained from a Millipore Milli-Q™ water system. A volume of 500 mL of this solution was used for each experiment. The pH of the solution was monitored throughout the experiment with a Bach-Simpson Ltd. pH 82 Standard pH meter with an Orion Research Ross pH Electrode. Solution pH values were obtained by transferring the electrode from a pH 4.0 buffer solution to the leaching solution and measuring the pH within 1 min, after which the electrode was returned to the buffer to prevent irreversible reactions at the electrode surface. The pH meter

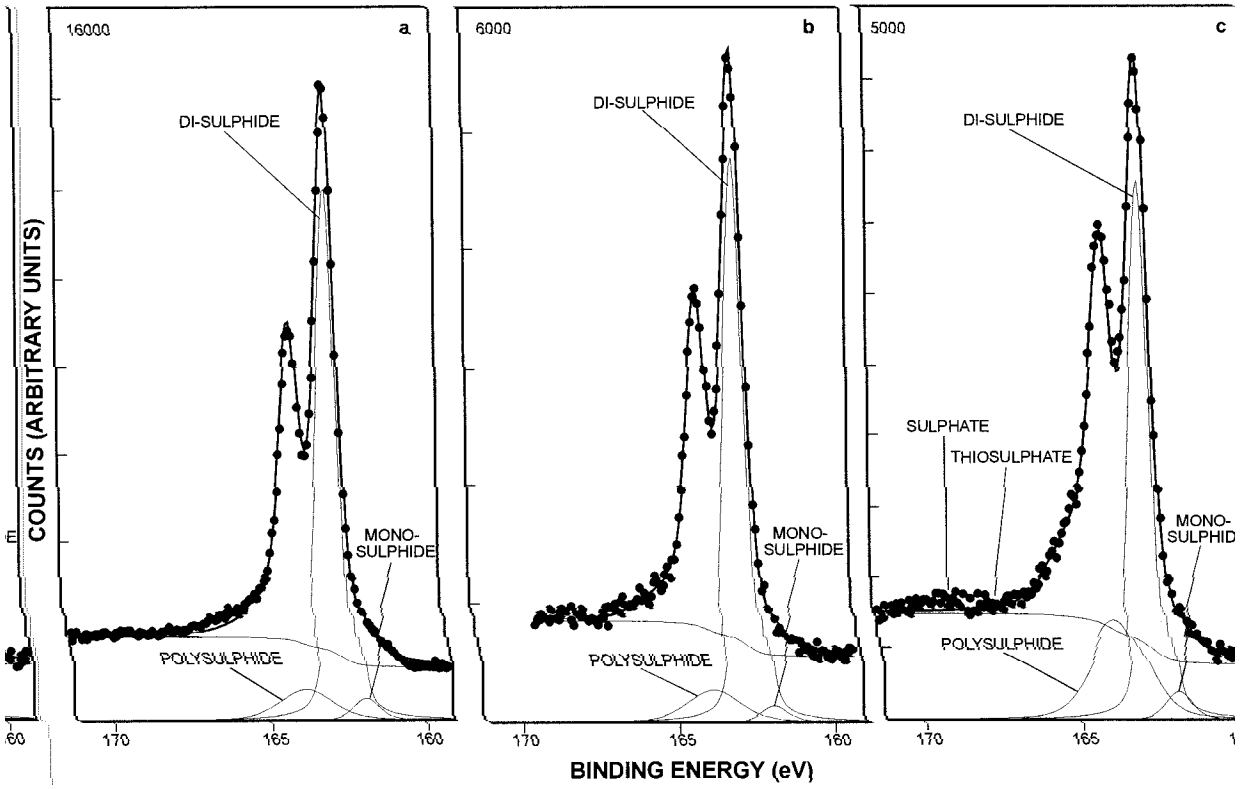

FIGURE 1. $S(2p_{3/2})$ XPS spectra of marcasite for (**a**) the pristine, vacuum-fracture surface; (**b**) the surface cleaned with boiling concentrated HCl for 15 min; and (**c**) the surface reacted in oxygenated and mildly acidic (pH = 3.0) solution for 6 h.

was calibrated using pH 4.10 and pH 2.00 buffers immediately before the experiment.

Experimental procedure. Dissolution experiments were carried out using a 500 mL batch reactor with a top-mounted impeller that sufficiently stirred the solution (at 900 rpm) to suspend the marcasite particles. The spinning impeller prevented abrasion of the marcasite grains that would occur if a Teflon-coated magnetic stir bar were used. A vortex was created by the spinning impeller that kept the solution aerated and therefore saturated with respect to O. Experiment solution temperatures were controlled at 25 ± 0.5 °C and 35 ± 0.5 °C using a LAUDA MT circulation heat pump immersed in a water bath. Temperatures were monitored throughout the experiment with a laboratory thermometer. Experiment solutions were assayed at appropriate intervals during the experiment by removing 6 mL aliquots; 5 and 1 mL portions were used for Fe and S analyses, respectively. Each sample was immediately filtered using a 0.2 μm pore membrane filter to remove any suspended particles. Correction for change in volume of solution, because of sampling, was made for each experiment.

Fe analyses were achieved using a Milton Roy Company Spectronic 20D colorimetric spectrometer. Fe^{3+} was measured within 5 min of removing the sample using colorimetric measurements with ammonium thiocyanate as an indicator (Sandell 1944). Two drops of H_2O_2 were subsequently added to the aliquot to oxidize Fe^{2+} to Fe^{3+} and the analysis was repeated resulting in a measurement of total Fe. Ion chromatography was used for the measurements of SO_4^{2-} and total S in solution. S analyses were obtained within 10 min of sample removal. The instrument used for chromatography was a Dionex DX-100 ion chromatograph with conductivity detection. A Dionex AS4A column was used with a CO_3^{2-}/HCO_3^- eluent at 2 mL/min. SO_4^{2-} was determined initially (retention time of 4.5 ± 0.05 min), and total reactive sulfur was determined by repeating the procedure after introducing two drops of H_2O_2 to the aliquot. Standards were prepared using ACS reagent-grade chemicals.

RESULTS

Surface analyses

XPS and AES results are presented in Figures 1–4 and the peak parameters for the XPS results are listed in Table 2. Eight electron microprobe analyses of marcasite show the sample to contain 33.52 (s = 0.20) and 66.46 (s = 0.21) atom% Fe and S, respectively. Irregular (less than 0.05 atom%) occurrences of Co and Ni were also detected. The S/Fe ratio of 1.98 atom% is very close to the idealized FeS_2 composition (S/Fe ratio = 2.00). XRF results detect Cu (200 ppm), Ni (650 ppm), and trace amounts (< 100 ppm) of Zn, As, and Mn.

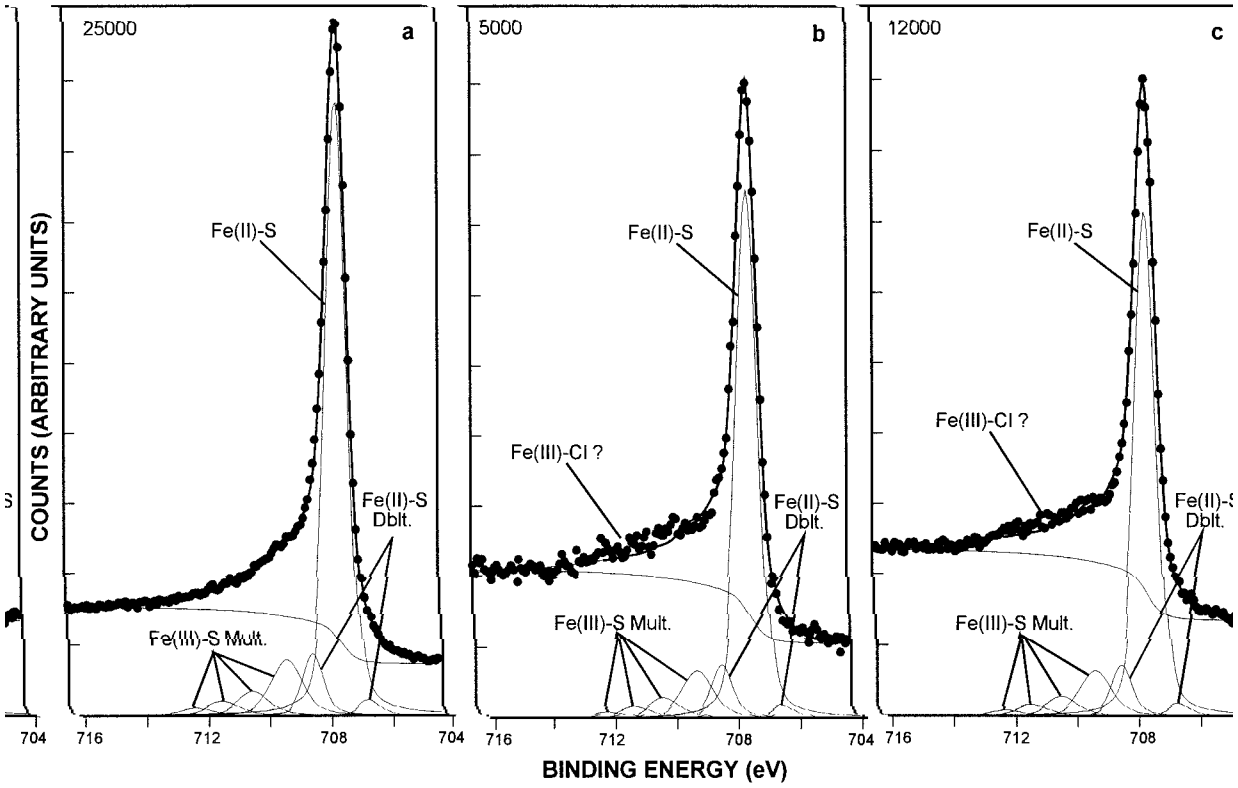

FIGURE 2. Fe(2p) XPS spectra of marcasite for (**a**) the pristine, vacuum-fracture surface; (**b**) the surface cleaned with boiling concentrated HCI for 15 min; and (**c**) the surface reacted in oxygenated and mildly acidic (pH = 3.0) solution for 6 h.

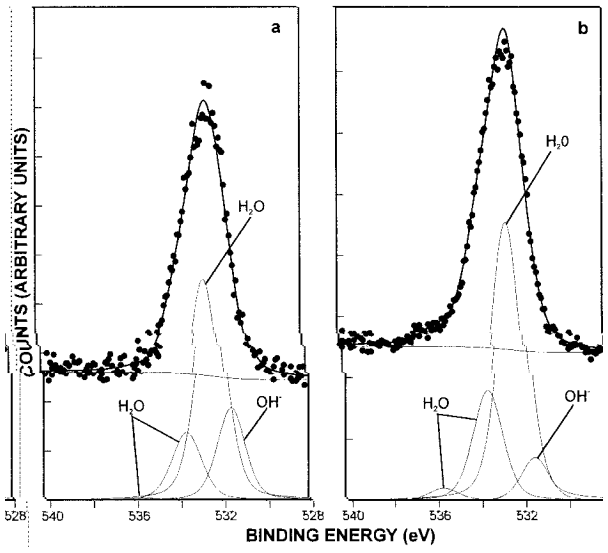

FIGURE 3. O(1s) XPS spectra of marcasite for (**a**) the surface cleaned with boiling concentrated HCI for 15 min and (**b**) the surface reacted in oxygenated and mildly acidic (pH = 3.0) solution for 6 h.

XPS broadscan spectra yields an S/Fe ratio of 2.81, 2.15, and 2.91 for the vacuum-fractured, the cleaned, and the reacted surfaces, respectively (Table 3), whereas AES analyses of the reacted marcasite surface yields an S/Fe ratio of 2.00 (Table 3). The XPS broadscan analyses of the vacuum fractured, cleaned, and reacted marcasite surfaces yield an anomalously large S content. There is no explanation for the anomalous result; however, other studies (McIntyre et al. 1996; Nesbitt et al. 1995; Nesbitt and Muir 1994; Pratt et al. 1994a; Mycroft et al. 1990) with Ni, Co, As, and Fe sulfides obtained similar results. XPS broadscan analyses also reveal the presence of chloride on the surfaces exposed to HCl.

Aqueous analyses

Total dissolved Fe(aq) for all experiments are plotted in Figures 5a, 5b, and 5c. Dissolved S concentrations for both surface-prepared and untreated experiments are plotted for 25 °C in Figures 5d, 5e, and 5f. Fe(aq) speciation is plotted for both surface prepared and untreated experiments at 25 °C in Figure 6. Experimental rate coefficients and apparent activation energies (E_a) are listed in Table

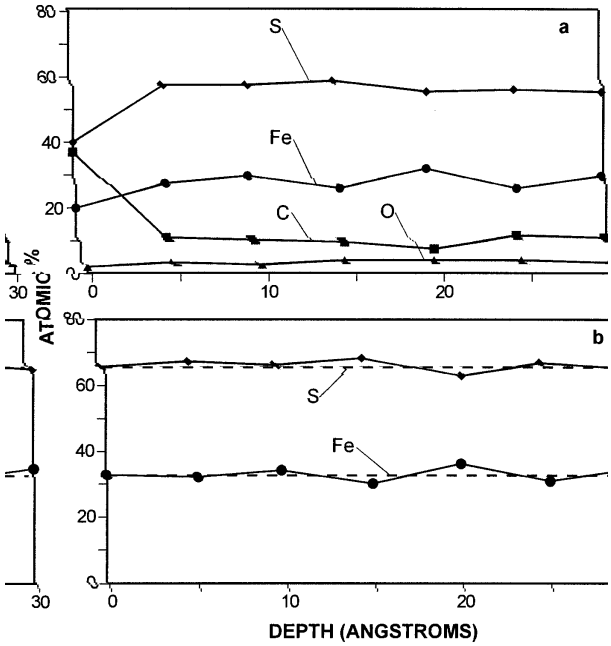

FIGURE 4. AES depth profile of marcasite surface reacted in oxygenated and mildly acidic (pH = 3.0) solution for 6 h. (**a**) Includes contamination of C and O (**b**) C and O are normalized out of data. Dashed line represents a pristine marcasite surface.

4. The early stages of Fe leaching from untreated marcasite in oxygenated mildly acidic solutions are apparently governed by the rate law:

$$d[Fe]/dt = (2.21 \times 10^{-2})\ t^{-0.5} \quad (4)$$

where [Fe] represents the concentration of Fe (mmol), t is time (s) and 2.2×10^{-2} is the rate coefficient in mmol/$s^{1/2}$. The early stages of Fe leaching from pristine marcasite in oxygenated mildly acidic (pH 3.0) solution are governed by the rate law:

$$[Fe] = [Fe]_0 + (4.25 \times 10^{-5})\ t \quad (5)$$

where [Fe] is the aqueous concentration of Fe (mmol), t is time (s) and 4.25×10^{-5} is the rate coefficient (mmol/s) and $[Fe]_0$ is the initial concentration of Fe (mmol).

The pH of the solutions changed ± 0.04 pH units during the 6 h experiment and may result from drift of the instrument. Comparisons made between the solubility product for marcasite (Schoonen and Barnes 1991) and the ion activity product (IAP) calculated for experimental solutions suggest that these solutions remain grossly undersaturated with respect to marcasite during the course of all experiments.

INTERPRETATION

Surface analyses: Peak identification

Details of fitting the S(2p), Fe(2p), and O(1s) spectra and refinements to peak parameters are discussed by Nesbitt and Muir (1994).

S(2p) spectra. Buckley and Woods (1987), Mycroft et al. (1990), and Nesbitt and Muir (1994) observed the disulfide (S_2^{2-}) peak for pyrite at 162.40 ± 0.10 eV. The major peaks of Figures 1a, 1b, and 1c are at 162.42 eV and are likewise interpreted as the disulfide peak for marcasite. Buckley and Woods (1987), Mycroft et al. (1990), Pratt et al. (1994a), and Nesbitt and Muir (1994) observed a peak located at approximately 1 eV lower binding energy than the disulfide peak and interpreted it to be monosulfide (S^{2-}). The minor peak at 161.69 eV (Figs. 1a and 1b) and at 161.67 eV (Fig. 1c) occurs at 0.7 eV lower binding energy than the disulfide peak and is interpreted to be the monosulfide peak for marcasite. An additional peak at 163.62 eV in Figures 1a and 1b and at 163.5 eV in Figure 1c is interpreted to be polysulfide ($S_2^{2-} - S_7^{2-}$), which is consistent with the interpretations of others with pyrite (Hyland and Bancroft 1989; Mycroft et al. 1990; Nesbitt and Muir 1994). The S(2p) signal between 166 and 170 eV (Fig. 1c) is slightly elevated over the background but no distinct peaks are observed. This is discussed further during interpretation of spectral changes caused by reactions with oxygenated HCl solution (pH 3.0).

Fe(2p) spectra. Buckley and Woods (1987), Mycroft et al. (1990), and Nesbitt and Muir (1994) determined binding energies for the Fe^{2+} peak of the Fe($2p_{3/2}$) spectrum of pyrite at 707.0 ± 0.1 eV and interpreted this peak

TABLE 2. XPS peak parameters and chemical states of S, Fe, and O for marcasite surfaces

Spectrum	B.E. (eV)	FWHM	Percentage of species detected: Vac.-Frac.	6 h reacted	Cleaned	Comments
S(2p)	161.69	1.0	4.54	4.50	3.26	Monosulphide
	162.87	1.0				Doublet*
	162.44	0.75	82.94	64.37	84.20	Disulphide
	163.62	0.75				Doublet*
	163.62	2.0	12.52	0.00	12.54	Polysulphide†
	164.80	2.0				Doublet*
	163.50	2.0	0.00	31.13	0.00	Polysulphide‡
	164.68	2.0				Doublet*
Fe(2p)	708.10	0.82				Fe^{2+}-S Multiplet
	707.20	0.82	83.0	79.0	78.0	Fe^{2+}-S Major
	706.30	0.82				Fe^{2+}-S Multiplet
	713.05	2.2				Fe^{2+}-Satellite
	708.95	1.2	17.0	4.0	5.0	Fe^{3+}-S Major
	710.05	1.2				Fe^{3+}-S Multiplet
	711.05	1.2				Fe^{3+}-S Multiplet
	711.95	1.2				Fe^{3+}-S Multiplet
	709.00	1.2	0.0	10–15	10–15	Fe^{3+}-? Major§
	710.00	1.2				Fe^{3+}-? Multiplet
	711.10	1.2				Fe^{3+}-? Multiplet
	712.15	1.2				Fe^{3+}-? Multiplet
O(1s)	531.32	1.5	—	9.10	23.00	Hydroxide
	532.30	1.6	—	63.12	58.00	Attached H_2O
	533.48	1.6	—	25.00	18.40	Adsorbed H_2O
	535.50	1.6	—	2.78	0.66	Adsorbed H_2O

* Each doublet is associated with the peak listed above it, and the peak area of each doublet is included in the peak area with the associated main peak.

† Polysulphide associated with vacuum fractured marcasite only.

‡ Polysulphide associated with the marcasite surface reacted in oxygenated and acidified solution only.

§ Postulated species (see text).

TABLE 3. XPS and AES analyses of marcasite in atomic percent and ratios of surface atoms determined from broadscans

	Experimental conditions	Fe(3p)	S(2p)	O(1s)	C(1s)	Cl(1s)	O/Fe	S/Fe	O/S
XPS	Vacuum-fractured	19.53	54.84	0.85	23.59	0.00	0.04	2.81	0.02
	6 h in HCl (pH = 3.0)	7.63	22.18	15.96	52.65	1.13	2.09	2.91	0.72
	Cleaned in conc. HCl	9.39	20.18	9.43	54.95	6.04	1.00	2.15	0.47
		Fe_{kll}	S_{kll}	O_{kll}	C_{kll}		O/Fe	S/Fe	O/S
AES	6 h in HCl (pH = 3.0)	20.0	40.0	2.1	37.0	—	0.11	2.00	0.05

to be Fe^{2+} bonded to S. Multiplet contributions were calculated for the Fe^{2+} free ion (Gupta and Sen 1975) relative binding energies and peak intensities contributing to the Fe($2p_{3/2}$) spectrum. Pratt et al. (1994a) and Nesbitt and Muir (1994) used these theoretical results as a guide to fitting the Fe(2p) spectrum. Their results were used here to interpret the Fe(2p) spectrum of marcasite. The main peak for Fe^{2+} of the fresh, cleaned, and reacted surfaces is located at 707.20 eV with two minor multiplets fitted at 706.30 and 708.10 eV. These peaks are here interpreted to be Fe^{2+} bonded to S. There is a large high energy tail in the Fe(2p) spectrum (708.95 eV), which may represent Fe^{3+} bonded to S (Nesbitt and Muir 1994). The cleaned and reacted surface Fe(2p) spectrum (Figs. 2b and 2c) cannot be fit using the same constraints as the fresh surface (Fig. 2a). An additional peak at approximately 709.00 eV with multiplets at 710.00 eV, 711.10 eV, and 712.15 eV must be included to obtain a good fit.

O(1s) spectra. Nesbitt and Muir (1994) reported an O(1s) peak at 532.4 eV on pyrite and interpreted it to be chemically attached H_2O. The cleaned marcasite O(1s) spectrum (Fig. 3a) and the reacted marcasite O(1s) spec-

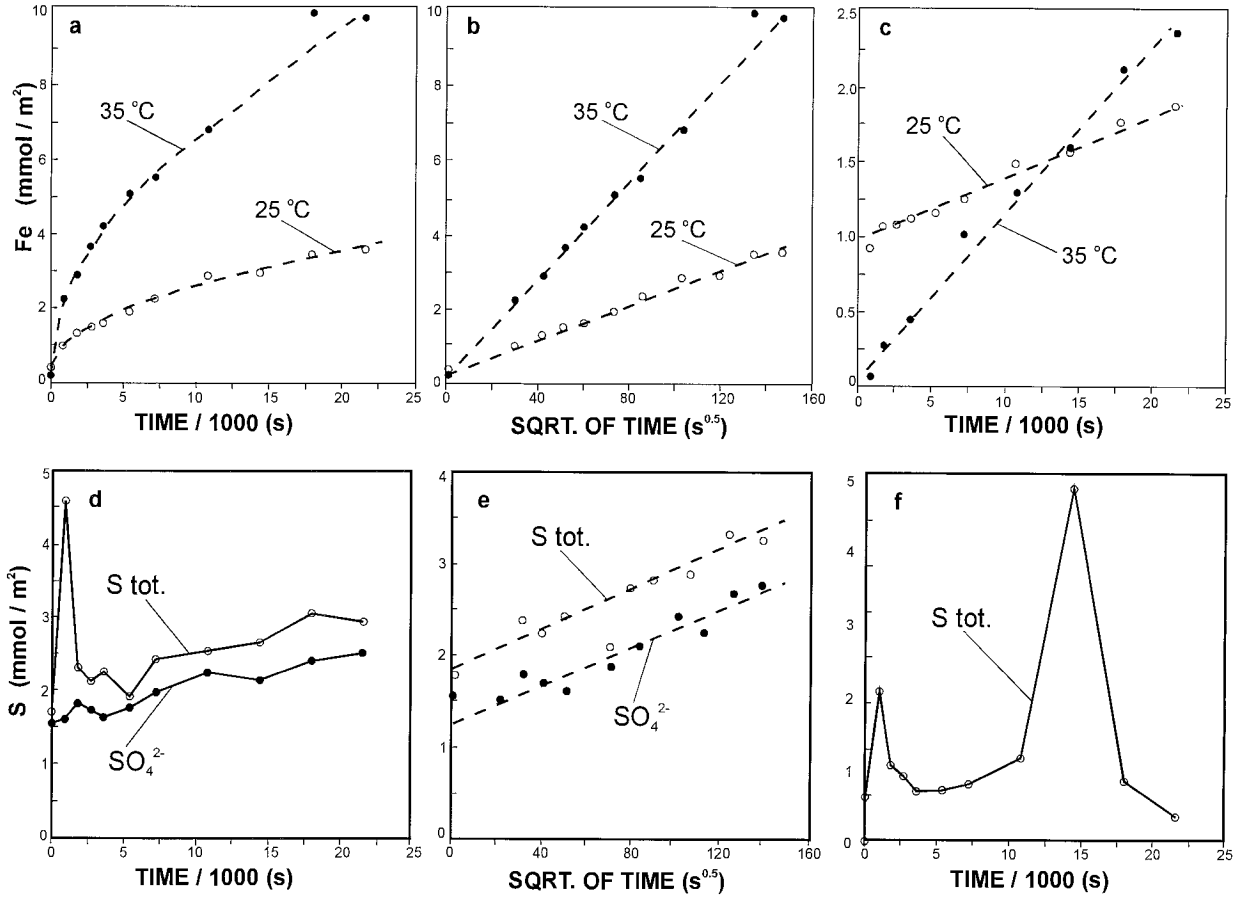

FIGURE 5. Aqueous plots of marcasite oxidative dissolution in oxygenated and mildly acidic (pH = 3.0) solution. (**a**) Fe leached from untreated samples at 25 and 35 °C plotted against time. (**b**) Fe leached from untreated samples at 25 and 35 °C plotted against the square root of time. (**c**) Fe leached from cleaned samples at 25 and 35 °C plotted against time. (**d**) SO_4^{2-} and S_{tot} leached from untreated samples at 25 °C plotted against time. (**e**) SO_4^{2-} and S_{tot} leached from untreated samples at 25 °C plotted against the square root of time. (**f**) S_{tot} leached from treated samples at 25 °C plotted against time.

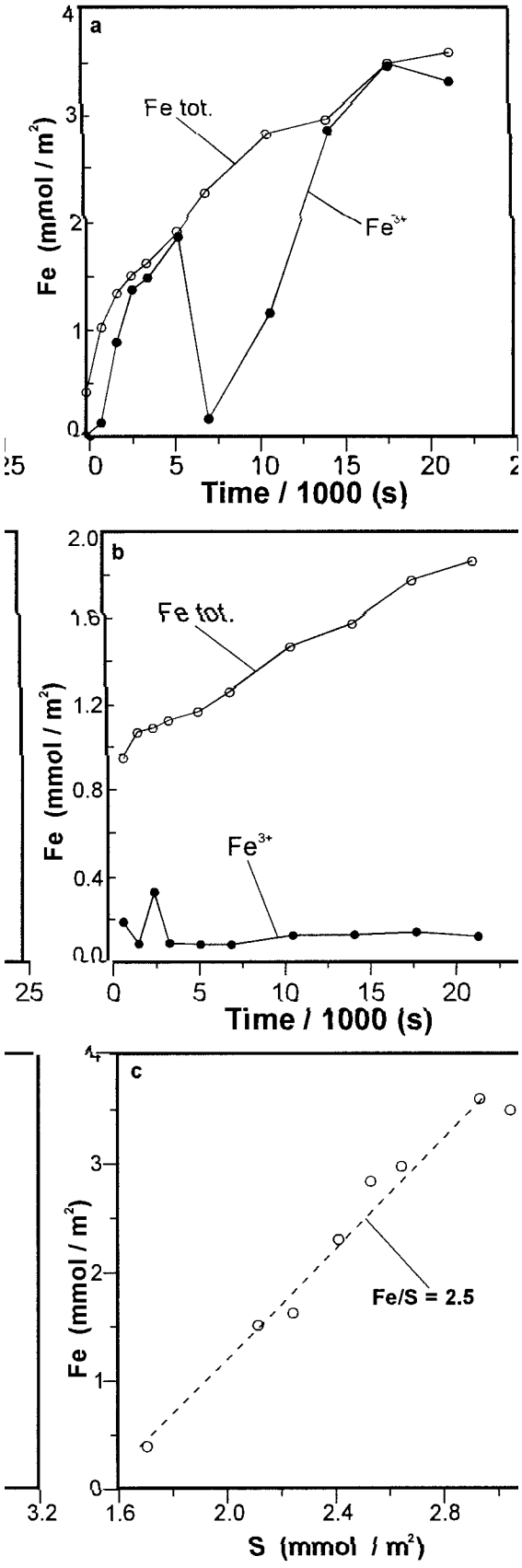

FIGURE 6. Aqueous Fe speciation. (**a**) Leached from untreated marcasite samples at 25 °C in oxygenated and mildly acidic (pH = 3.0) solution and (**b**) leached from cleaned marcasite samples in oxygenated and mildly acidic (pH = 3.0) solution. (**c**) Fe vs. S_{tot} leached from oxygenated and mildly acidic (pH = 3.0) solution at 25 °C. The pulse of S (see text) was removed from the data.
←

trum (Fig. 3b) also have a peak at 532.4 eV, which we interpret to be H_2O chemically attached to the marcasite surface. McIntyre and Zetaruk (1977), Mills and Sullivan (1983), and Nesbitt and Muir (1994) reported a hydroxide peak at 531.4 eV. A small peak at 531.32 eV is required to fit the O(1s) spectrum and is interpreted to be an hydroxide species. Knipe et al. (1995) observed O(1s) peaks at 533.50 eV and 535.50 eV and interpreted them as physically adsorbed H_2O and hydroxyl radicals in poor electrical contact with the mineral surface. The peaks at 533.48 eV and 535.50 eV (Figs. 3a and 3b) were interpreted similarly.

Spectral changes because of cleaning with concentrated HCl

S(2p) spectra. No observed changes exist in the S(2p) spectrum (Figs. 1a and 1b) for disulfide during exposure of the cleaved face to boiling concentrated HCl for 15 min. Disulfide is the major peak of the S(2p) spectra for both the vacuum-fractured and the cleaned surfaces and its signal remains constant at 83 ± 2% of total S during reaction with concentrated HCl (Table 3, Figs. 1a and 1b). Polysulfide and monosulfide also remain constant at 12.5 ± 2% and 4.5 ± 2% of total S, respectively, on the fresh and cleaned surface.

Fe(2p) spectra. Minor changes are observed in the Fe(2p) spectrum during exposure of the fresh surface to boiling concentrated HCl for 15 min. The Fe^{2+} S peak (707.20 eV) decreases from 83 ± 2% on the fresh surface to 78 ± 2% on the cleaned surface (Table 3, Figs. 2a and 2b). The spectra of Fe^{3+} bonded to S decreases from 17 ± 2% on the fresh surface to 5 ± 2% on the cleaned surface. The Fe(2p) spectrum of the vacuum-fractured surface (Fig. 2a) is used as a template to discern any

TABLE 4. Experimental rate coefficients for various specimens

Experiment no.	k_p (25 °C) (mmol/m²·S$^{0.5}$)	k_p (35 °C) (mmol/m²·S$^{0.5}$)	E_a (kJ/mol)
1*	1.97×10^{-2}	4.98×10^{-2}	71
2*	2.28×10^{-2}	5.04×10^{-2}	67
3*	2.37×10^{-2}	5.69×10^{-2}	61
Avg.*	2.21×10^{-2} (mmol/m²·s)	5.24×10^{-2} (mmol/m²·s)	66
1†	4.25×10^{-5}	1.08×10^{-4}	71

Notes: Rates are adjusted for surface area at temperatures of 25 and 35 °C. Activation energies are obtained from an Arrhenius plot of the results.
* Specimens were not cleaned before the experiment.
† Specimen was vigorously cleaned before the experiment.

further changes because of cleaning. This determination is achieved by placing the fitted curve of the vacuum fracture surface over the data obtained from the surface exposed to concentrated HCl solution (Fig. 2b). The data between 709 and 712 eV plot above the fitted curve of the vacuum-fractured Fe(2p) spectrum, and the counts integrated over this energy range represent 10–15% of the total Fe counts.

The peak found within the energy range of 709 and 712 eV is too low to be interpreted as an Fe^{3+}-O contribution such as observed for goethite (Fe-O-OH), and is too high to result from Fe^{3+}-S such as observed in the spectrum of the vacuum-fractured surface. The remaining possibilities are Fe^{2+}-O, Fe^{3+}-OH, or Fe^{3+}-Cl surface species.

O(1s) spectra. Nesbitt and Muir (1994) have demonstrated that O contamination in the XPS vacuum chamber is negligible in comparison with exposure to H_2O vapor. It is assumed here that O species found on the reacted face are derived from the concentrated HCl solution. The O(1s) spectrum of the cleaned marcasite surface (Fig. 3a) shows a 59 ± 2% contribution to the O (1s) spectra from chemically attached H_2O (B.E. = 532.30 eV) and a smaller proportion of physically absorbed H_2O that contributes 19 ± 2% total O (B.E. = 533.48 and 535.50 eV). The hydroxyl ion (B.E. = 531.32 eV) contributes 23 ± 2% to the O (1s) spectrum. The absence of O^{2-} demonstrates that Fe^{2+}-O species are not present. The high concentration of OH^- on the reacted surface makes the presence of Fe^{3+}-OH surface species possible. The remaining possibility for the elevated signal between 709 and 712 eV of the Fe(2p) spectrum of the cleaned surface is an Fe^{3+}-Cl surface species. Support for a Fe^{3+}-Cl surface species derives from the broadscan results that indicate the presence of 5–10% Cl on the surface.

Spectral changes because of reaction with oxygenated HCl solution (pH 3.0)

S(2p) spectra. Significant changes were observed in the S(2p) spectrum (Figs. 1a and 1c) for disulfide during exposure of the cleaved face to oxygenated and mildly acidic (pH 3.0) solution. Disulfide is the major peak of the S(2p) spectrum for both the reacted and unreacted surfaces but its signal decreases from 83 ± 2% to 64 ± 2% of total S during reaction with the solution (Table 3, Figs. 1a and 1c). Polysulfide increases from 12.5 ± 2% on the fresh surface to 31 ± 2% on the reacted surface. Monosulfide remains constant at 4.5 ± 2% S. The results indicate that 19% of disulfide on the fresh surface is oxidized to polysulfides during exposure to oxygenated and acidified solution. This increase in polysulfide percentage is accompanied by a shift in polysulfide binding energy from 163.62 eV (fresh surface) to 163.5 eV (reacted surface). The shift toward the disulfide peak (162.4 eV) may indicate a change in polysulfide composition toward a lower average number of S atoms per unit polysulfide (e.g., $S_5^{2-} \rightarrow S_4^{2-}$); presumably the disulfide reaction products are primarily S_3^{2-} or S_4^{2-}, shifting the ''average'' to a value nearer S_3^{2-} or S_4^{2-}.

Although the portion of the S(2p) spectrum between 165–170 eV (Fig. 1c) is noisy, it is evident that there is little sulfate (~169 ± 1 eV) or thiosulfate (~167 ± 1 eV) present in the near surface. Thiosulfate has a low binding energy peak near 162 eV, which is the same intensity as the higher B.E. peak. If thiosulfate is present, the small contribution of the low energy peak makes an insignificant contribution to the polysulfide signal observed in Figure 1c.

Fe(2p) spectra. Minor changes are observed in the Fe(2p) spectrum after exposure of the fresh surface to the mildly acidic oxygenated solution for 6 h. The Fe^{2+}-S peak (707.2 eV) decreases from 83 ± 2% on the fresh surface to 79 ± 2% on the reacted surface (Table 3, Figs. 2a and 2b). The spectra of Fe^{3+} bonded to S decreases from 17 ± 2% on the fresh surface to 4.6 ± 2% on the reacted surface. The Fe(2p) spectrum of the vacuum-fractured surface (Fig. 1a) is used as a template to investigate additional changes to the Fe(2p) of the reacted surface (Fig. 1c). The data between 709 and 712 eV plot above the fitted curve from the vacuum-fractured Fe(2p) spectrum and the counts integrated over this energy range represent 10–15% of the total Fe counts. This species is likely to be the same species found on the surface exposed to boiling concentrated HCl. Broadscan results of this surface indicate a small amount of Cl on the reacted surface.

O(1s) spectra. The O(1s) spectrum of the reacted marcasite surface (Fig. 3b) shows a large contribution to the O(1s) spectra from chemically attached water of 63 ± 2% (B.E. = 532.30 eV) and a smaller proportion of physically absorbed water (B.E. = 533.48 and 535.50 eV) that contributes 28 ± 2%. The hydroxyl ion (B.E. = 531.32 eV) contributes 9 ± 2% to the O(1s) spectrum. In comparison with the spectrum obtained from the marcasite surface cleaned in concentrated HCl, the attached H_2O species increased at the expense of the hydroxyl ion. There can be no significant contribution of O from sulfate or thiosulfate to the O(1s) spectrum because, if present, their abundance in the near surface is very low (Fig. 1c). The absence of an oxide peak indicates that no Fe^{3+}-oxyhydroxides have formed. The hydroxide may represent Fe^{3+}-hydroxide in the near-surface, but another explanation related to reaction mechanism is offered in the discussion.

AES data

An AES depth profile of marcasite reacted in HCl (pH 3.0) for 6 h is illustrated in Figure 4a. The profile does not indicate the presence of an oxidized or compositionally distinct near-surface zone. Whereas XPS broadscan analysis suggests that Fe may be depleted on the surface this is not seen on the profile. C contaminated the surface and the escape depth of Auger electrons ejected from a solid varies with individual elements. The escape depth of Auger electrons from S is shallower than those from

Fe. Correction for the attenuation by the monolayer of C was made by inserting values obtained from the integrated form of the AES survey scan that was obtained before sputtering. Figure 4b illustrates the AES depth profile for S and Fe with C and O normalized out of the analyses. The dashed lines of Figure 4b represent an idealized marcasite composition and illustrate that the S/Fe ratio of the reacted sample is effectively the same as that for an unreacted sample.

Leaching studies: 25 °C

Untreated marcasite. Fe concentrations plotted against time yield nonlinear trends (Fig. 5a), but plotted against the square root of time yield linear trends (Fig. 5b) for all experiments involving the untreated marcasite samples. The input rate of Fe to solution at 25 °C is 0.0221 ± 0.003 mmol/($m^2 \cdot s^{0.5}$) total Fe averaged over three experiments (Table 4). The linear trend obtained when data are plotted against the square root of time suggests that diffusion controls the rate of release of Fe from the solid (Pratt 1995; Wollast 1967).

Total aqueous Fe and Fe^{3+} species have been plotted as a function of time (Fig. 6a). Fe^{3+} dominates initially; however, a cyclical relationship exists where Fe^{2+} and Fe^{3+} are alternately dominant. This alternation was observed in all experiments, but not always at the same time. This effect was noted by others (R. Smart, personal communication). Congruent dissolution of marcasite should produce solutions with 100% of total dissolved Fe as Fe^{2+}. Oxidation of Fe^{2+}(aq) to Fe^{3+}(aq) is very slow at pH 3.0 in oxidized solutions (Singer and Stumm 1970), hence Fe^{3+} must be derived from the surface of the crushed marcasite. Additional experiments are necessary to investigate the source of Fe^{3+}.

S is present in solution (Fig. 5d) as both SO_4^{2-} and a less oxidized species of S immediately after leaching commences. The results indicate a significant release of S at approximately 15 min reaction time. Like Fe^{3+}, it may have been produced during crushing. This initial rapid aqueous release is from a S species of oxidation state lower than SO_4^{2-}. When the rapid increase is removed from the data, a near linear trend is observed for SO_4^{2-} and total S whether plotted against time (Fig. 5d) or the square root of time (Fig. 5e). As with Fe, a rate constant for the release of S to solution is determined and suggests that S is released into solution at a rate of 2.57×10^{-2} mmol/($m^2 \cdot s^{0.5}$) total S. The fate of the reduced S peaks is discussed subsequently.

A plot of S vs. Fe (Fig. 6c) gives a linear relationship with an atomic Fe/S ratio of 2.5 rather than the stoichiometric ratio of 0.5. Either Fe is preferentially released to solution or S release is retarded at the surface during reaction.

Surface-prepared marcasite. The analysis of total dissolved Fe for surface-treated samples demonstrate linear trends with respect to time (Fig. 5c). The rate of input of Fe to solution at 25 °C is 4.25×10^{-5} mmol/($m^2 \cdot s$) (Table 4). Analysis of aqueous Fe speciation (Fig. 6b) indicates that Fe exists as Fe^{2+} with minor (< 0.5 mmol) Fe^{3+}, which remains largely unchanged during the course of the experiment. The dominance of Fe^{2+} suggests that the source of Fe^{3+} was removed from the marcasite surface and that the leaching rate is the rate of oxidative dissolution of pristine marcasite.

The analysis of dissolved S (Fig. 5f) reveals no predictable trend for S leaching. There are two very high concentrations of aqueous S after 30 min and 5 h reaction time. These anomalous concentrations appear and disappear in a manner similar to that in the experiment where untreated samples were used. The results suggest that the pulse of S into solution is a function of the oxidation mechanism of marcasite rather than the result of oxidation products created at the surface during grinding.

Leaching studies: 35 °C

Untreated marcasite. Fe concentrations plotted against time yield parabolic trends (Fig. 5a), but plotted against the square root of time (Fig. 5b) yield linear trends for all experiments involving the untreated marcasite samples. The leaching rate of Fe from the untreated marcasite sample at 35 °C is 0.0524 ± 0.004 mmol/($m^2 \cdot s^{0.5}$) total Fe averaged over three experiments (Table 4).

Surface prepared samples. Iron concentrations plotted against time yield linear trends for all experiments involving pretreated marcasite samples (Fig. 5c). The rate of input of Fe into solution from the pretreated samples at 35 °C is 1.08×10^{-4} mmol/($m^2 \cdot s$) of total Fe (Table 4).

Kinetic aspects

Rate law. Aqueous Fe_{total} concentrations when plotted against the square root of time yield linear trends for the first few hours of all leaching experiments using untreated marcasite (Fig. 3a). Apparently the early stages of Fe leaching from crushed marcasite are governed by a parabolic rate law (Eq. 4). The integrated form of the rate law is:

$$[\mathrm{Fe}] = [\mathrm{Fe}]_o + \frac{2k_p}{\sqrt{t}} \quad (6)$$

where $[Fe]_o$ is the concentration of Fe in solution when the experiment begins. Rate coefficients, k_p (Table 4), were calculated from the slopes defined by the first 6 h of each experiment (Fig. 5b) and have been corrected to 1 L of solution and 1 m^2 of marcasite surface available to react.

A parabolic rate law in this case may not indicate that diffusion controls the release rate of Fe, but that strained or broken bonds created during grinding and smaller marcasite particles electrostatically adhered to the marcasite surface cause an initially high reaction rate. The reaction rate decreases with time as the smaller particles are dissolved and surface defects are removed from the surface. The apparent parabolic rate law found here for untreated

marcasite is applicable to crushed marcasite prepared for mineral processing in a ball or rod mill. The linear rate law for pristine marcasite leaching may be concealed. It may be applicable only after long reaction times, or it may never be applicable depending upon the effects of iron oxide coatings that develop on sulfides of mine wastes.

Aqueous Fe concentrations derived by leaching treated marcasite yield linear trends when plotted against time. Apparently the early stages of Fe leaching from crushed marcasite are governed by a linear rate law (Eq. 5). Pretreatment removed small grains attached to the surface and removed strained or broken bonds on the surface created during grinding. The rate coefficient was calculated from the slope determined by the first 6 h of each experiment (Fig. 5c) and was corrected to 1 L of solution and 1 m^2 of marcasite surface available to react.

Activation energies. The temperature dependence of the reaction rate coefficients were calculated by assuming that an Arrhenius relationship occurs between 25 °C and 35 °C. An apparent activation energy of 66 ± 5 kJ/mol was determined for the untreated marcasite samples (Table 4) and an apparent activation energy of 71 kJ/mol was determined from the pretreated marcasite samples (Table 4) within this temperature range. These relatively high activation energies suggest that the rate-limiting step is the destruction of relatively strong covalent bonds on the marcasite surface.

Discussion and conclusions

Marcasite surface analyses after cleaning

XPS broadscan analysis detect significant amounts of chloride on the mineral surface (6%). Chloride undoubtedly originates from the HCl solution; however, it is not clear how it is attached to the marcasite surface. The S(2p) spectra of the cleaned surface (Fig. 1b) reveals little change during the cleaning procedure. The Fe(2p) spectrum of the cleaned surface (Fig. 2b) also yields little change during reaction, although a new species appears at binding energy 709 to 712 eV, possibly an iron chloride surface complex. The O(1s) spectra of the cleaned surface (Fig. 3a) illustrates that H_2O and OH^- are present on the surface and the 709–712 eV peak of the Fe(2p) spectrum may result from Fe^{3+}-OH surface species.

Marcasite surface analyses after reaction in oxygenated HCl solution (pH 3.0)

XPS broadscan analysis detect trace amounts of chloride (< 2%). Examination of the S(2p) spectrum of the surface reacted with air-saturated HCl-solution of pH 3.0 (Fig. 1c) reveal that disulfide is oxidized to a polysulfide after 6 h. The boiled solution, by contrast, is likely to be purged of dissolved O, and there is no evidence of an increased polysulfide on the cleaned mineral surface (Fig. 1b). Apparently, the increase in polysulfide on the surface reacted with air-saturated HCl solution is promoted by dissolved O. The Fe(2p) spectrum of the unreacted surface and the surface reacted in dilute HCl solution (Figs. 2a and 2c) reveal little change during reaction, although the surface species formed during cleaning (709 to 712 eV) also appears here. The O(1s) spectrum of the reacted surface (Fig. 3b) illustrates that H_2O and OH^- are present on the marcasite surface. $Fe^{3+}O$, $Fe^{2+}O$, and O bearing S species are absent from the vacuum fracture and reacted Fe (2p) and S (2p) spectra (Figs. 1a, 1c, 2a, and 2c) and O^{2-} is absent from the reacted O(1s) spectrum (Fig. 3b). Although SO_4 is the stable form of dissolved S in oxygenated solutions, there is either insufficient time for production of, or HCl inhibits formation of, sulfate. Polysulfides apparently are intermediate reaction products formed on the mineral surface (at least in the presence of HCl).

Nature of surface polysulfides

AES depth profiles indicate that oxidative dissolution of marcasite occurs stoichiometrically. There is no evidence of preferential removal of Fe from the marcasite lattice, as observed for pyrite (Sasaki et al. 1995). XPS data indicate a slight (negligible?) increase in the S/Fe ratio during reaction with oxygenated and acidified waters that is not seen by AES analysis and the enhanced S/Fe values may be the result of polysulfide or native sulfur (S_8^{2-}) formation on the surface. These must form, however, as islands and detected only by the large analytical area analyzed by XPS. They are not observed in the AES analyses with its 1 μm spot size (diameter).

Rates of reaction

The oxidation leach rate of Fe(aq) from cleaned marcasite is 4.25×10^{-5} mmol/(m^2·s) at 25 °C in solutions of HCl (pH 3.0) equilibrated with the atmosphere. The activation energy for the reaction is 71 kJ/mol. It was also demonstrated that the reaction proceeds non-stoichiometrically, with sulfur released from the marcasite surface in pulses rather than accumulating steadily in solution.

The oxidation leach rate of Fe(aq) from the untreated marcasite is 2.2×10^{-2} mmol/($m^2 \cdot s^{0.5}$) at 25 °C in solution of HCl (pH 3.0) equilibrated with the atmosphere. The activation energy for the reaction is 65 kJ/mol. Fe^{3+}(aq) is observed during the initial stages of the experiment. The pulses of sulfur observed during the experiment with cleaned marcasite samples are also observed here.

Mechanism of reaction

Goldhaber (1983) and McKibben and Barnes (1986) reported that the absence of Fe^{3+} in solution requires marcasite oxidation to be initiated by adsorption of O_2 onto the partially protonated surface. Moses et al. (1987) pointed out that there is a low probability for direct reaction between molecular O_2, which is paramagnetic, and a diamagnetic disulfide. Presumably, the mechanism of oxidation by adsorbed O must occur with O_2 accepting electrons, forming O^{2-} on the marcasite surface (Roberts 1991). Examination of the O (1s) spectra after 6 h exposure to an oxygenated and acidified solution (Fig. 3b) does not reveal O^{2-} on the marcasite surface. The peak

for adsorbed O_2 occurs at a binding energy of 532.5 eV (McIntyre and Zetaruk 1977). This peak is masked by peaks of chemically and physically attached H_2O that occur at 532.30 and 533.48 eV, respectively. The absence of attached or sorbed O species other than that of H_2O and hydroxyl makes it difficult to establish a direct mechanism of oxidation involving sorbed O_2. Clearly, however, O^{2-} does not form and any mechanism that proposes its formation during initial reaction is incorrect. If OH^- is the reaction product of sorbed O_2 according to:

$$½O_2^0 + H_2O + 2e\text{-} \rightarrow 2(OH) \quad (7)$$

as suggested by Nesbitt and Muir (1994) for pyrite then the oxidation of marcasite in the pH 3.0 solution is a surface reaction that proceeds with dissolved O as the electron acceptor (Eq. 7) and the probable electron donor is S_2^{2-} on the marcasite surface (Eq. 8).

$$2S_2^{2-} \rightarrow S_4^{2-} + 2e^- \quad (8)$$

This mechanism is supported by the presence of abundant polysulfide species on the marcasite surface reacted with air-saturated HCl solution, and their absence from the surface of marcasite reacted with boiling HCl solution (from which O_2 is purged). The apparent absence of oxide O^{2-} from the O(1s) spectrum may be also accounted for if the residence time of O^{2-} on the marcasite surface is not sufficiently long to be seen by XPS analyses.

This mechanism may be replaced by oxidation by Fe^{3+} (Eq. 2) in experiments where untreated marcasite samples were used; Fe^{3+} present on the mineral surface is immediately added to solution during leaching. By contrast, Fe^{3+} was not leached from surface prepared samples indicating that the Fe^{3+} surface complex observed during near surface studies is not active in promoting leaching.

The production of pulses of S during oxidation suggests that an unstable, S-rich, Fe deficient layer accumulates on the marcasite surface. This layer is periodically shed from the surface, resulting in the pulses of S. The disappearance of S in solution may be caused by evolution of a gas phase S species (H_2S), precipitation of S species (S°) or readsorption of S onto the marcasite surface. An alternative explanation for the behavior of aqueous S is based on near-surface analyses. The islands of polysulfide observed may be shed from the marcasite surface as colloids. These colloids are randomly picked up during aqueous sampling, resulting in pulses that appear and disappear.

Taylor et al. (1984) studied O and S isotope geochemistry of sulfides, sulfate, O, and H_2O. They report that dissolved O gas is the major source of O in oxidized S species produced from pyrite reacted with oxygenated and acidified solutions. Nicholson (1994) argued that fractional rate dependence implies reaction mechanisms involving control by sorption or desorption. Fractional rate dependence of pyrite oxidation on O concentration has been reported by Smith et al. (1968), McKibben and Barnes (1986), Nicholson et al. (1988), and Williamson and Rimstidt (1994). The mechanism of oxidation proposed here is consistent with their work. It is concluded that the oxidative dissolution of marcasite in oxygenated and mildly acidic (pH 3.0) solution proceeds by surface reactions involving adsorption of dissolved O onto the surface and subsequent oxidation of disulfide. Fe is released to solution upon oxidation. Disulfide is oxidized to polysulfide on the marcasite surface and accumulates as islands on the surface before being released into solution.

Effects of grinding

Grinding marcasite or milling it during mining operations creates an oxidized Fe coating on the marcasite surface. This coating provides Fe^{3+} to solution during oxidative dissolution and gives the appearance of an anomalously high reaction rate during the first 6 h of reaction time. The supply of Fe^{3+} to solution has implications for flotation processes and for reactivity of sulfides in mine waste dumps. Oxidation of FeS_2 by Fe^{3+} (Eq. 2) is an order of magnitude faster than oxidation by O_2 (Wiersma and Rimstidt 1984). Furthermore, oxidation by Fe^{3+} proceeds under aerobic or anaerobic conditions (Moses et al. 1987), thus, abatement programs that rely on the prevention of oxygenated conditions may have limited initial success where Fe^{3+} is available at crushed marcasite surfaces, through the dissolution of species created by grinding. Once Fe^{3+} is removed from the surface, abatement programs should perform as anticipated.

Acknowledgments

The authors thank R. Martin of the Department of Chemistry for generously sharing his IC facilities and expertise with us. Comments from reviewers C. Moses, K. Nagy, and one anonymous reviewer were beneficial to this manuscript. The electron microprobe analyses were conducted by E. Thilbeault, Department of Earth Sciences, University of Western Ontario. This research was conducted through financial support of NSERC grants.

References cited

Brown, A.D. and Jurinak, J.J. (1989) Mechanism of pyrite oxidation in aqueous mixtures. Journal of Environmental Quality, 18, 545–550.

Buckley, A.N. and Woods, R. (1987) The surface oxidation of pyrite. Applied Surface Science, 27, 437–452.

Chaney, R.L. (1987) Recent developments in spatially resolved ESCA. Surface and Interface Analysis, 10, 36–47.

Fleet, M.I. (1970) Structural aspects of the marcasite-pyrite transformation. The Canadian Mineralogist, 10, 225–231.

Garrels, R.M. and Thompson, M.E. (1960) Oxidation of pyrite by iron sulphate solutions. American Journal of Science, Bradley Vol. 258-A, 57–67.

Goldhaber, M.B. (1983) Experimental study of metastable sulfur oxyanion formation during pyrite oxidation at pH 6–9 and 30 °C. American Journal of Science, 283, 193–202.

Gupta, R.P. and Sen, S.K. (1975) Calculation of multiplet structure of core p-vacancy levels. Physics Reviews, 12, 15–19.

Hyland, M.M. and Bancroft, G.M. (1989) An XPS study of gold deposition at low temperatures on sulphide minerals: Reducing agents. Geochimica et Cosmochimica Acta, 53, 367–372.

Jambor, J.L. (1994) Mineralogy of sulphide-rich tailings and their oxidation products. In J.L. Jambor and D.W. Blowes, Eds., Environmental Geochemistry of Sulphide Mine-Wastes, 22, p. 59–102. Mineralogical Association of Canada.

Jones, C.F., Lecount, S., Smart, R., and White, T. (1992) Compositional

and structural alteration of pyrrhotite surfaces in solution: XPS and XRD studies. Applied Surface Science, 55, 65–85.

Knipe, S.W., Mycroft, J.R., Pratt, A.R., Nesbitt, H.W., and Bancroft, G.M. (1995) X-ray photoelectron spectroscopic study of water adsorption on iron sulphide minerals. Geochimica et Cosmochimica Acta, 59, 1079–1090.

Lowson, R.T. (1982) Aqueous oxidation of pyrite by molecular oxygen. Chemical Reviews, 82, 463–497.

McIntyre, N.S. and Zetaruk, D.G. (1977) X-ray photoelectron spectroscopic studies of iron oxides. Analytical Chemistry, 49, 1521–1529.

McIntyre, N.S., Davidson, R.D., and Mycroft, J.R. (1996) Quantitative XPS measurements of some oxides, sulphides and complex minerals. Surface and Interface Analysis, 24, 591–596.

McKibben, M.A. and Barnes, H.L. (1986) Oxidation of pyrite in low temperature acidic solutions: Rate laws and surface textures. Geochimica et Cosmochimica Acta, 50, 1509–1520.

Mills, P. and Sullivan, J.L. (1983) A study of the core level electrons in iron and its three oxides by means of photoelectron spectroscopy. Journal of Physics D: Applied Physics, 16, 723–732.

Moses, C.O., Nordstrom, D.K., Herman, J.S., and Mills, A.L. (1987) Aqueous pyrite oxidation by dissolved oxygen and by ferric iron. Geochimica et Cosmochimica Acta, 51, 1561–1571.

Moulder, J.F., Stickle, W.F., Sobol, P.E., and Bomben, K.D. (1992) ϕ Handbook of X-ray photoelcectron spectroscopy. Perkin Elmer Corporation.

Mycroft, J.R., Bancroft, G.M., McIntyre, N.S., Lorimer, J.W., and Hill, I.R. (1990) Detection of sulphur and polysulphides on electrochemically oxidized pyrite surfaces by X-ray photoelectron spectroscopy and Raman spectroscopy. Journal of Electroanalytical Chemistry, 292, 139–152.

Nesbitt, H.W. and Muir, I.J. (1994) X-ray photoelectron spectroscopic study of a pristine pyrite surface reacted with water vapour and air. Geochimica et Cosmochimica Acta, 59, 4667–4679.

Nesbitt, H.W., Muir, I.J., and Pratt, A.R. (1995) Oxidation of arsenopyrite by air and air-saturated, distilled water, and implications for mechanism of oxidation. Geochimica et Cosmochimica Acta, 59, 1773–1786.

Newhouse, W.H. (1925) Paragenesis of marcasite. Economic Geology, 26, 54–66.

Nicholson, R.V. (1994). Iron-Sulfide Oxidation Mechanisms: Laboratory Studies. In J.L. Jambor and D.W. Blowes, Eds., Environmental Geochemistry of Sulphide Mine-Wastes, 22, p. 163–183. Mineralogical Association of Canada,

Nicholson, R.V. Gillham, R.W., and Reardon, E.J. (1988) Pyrite oxidation in carbonate buffered solutions: 1. Experimental kinetics. Geochimica et Cosmochimica Acta, 52, 1077–1085.

Nordstrom, D.K. (1982) Aqueous pyrite oxidation and the consequent formation of sondary minerals, In Acid Sulphate Weathering, p. 37–46. Soil Science Society of America, Madison, Wisconsin.

Pratt, A.R. (1995) The low temperature surface geochemistry and kinetics of pyrrhotite weathering: Influences on acid mine drainage (AMD): Ph.D. thesis, University of Western Ontario, 182 p.

Pratt, A.R., Muir, I.J., and Nesbitt, H.W. (1994a) X-ray photoelectron and Auger electron spectroscopic studies of pyrrhotite and mechanism of air oxidation. Geochimica et Cosmochimica Acta, 58, 827–841.

———(1994b) Generation of acids form mine waste: oxidative leaching of pyrrhotite in dilute H_2SO_4 solutions at pH 3.0. Geochimica et Cosmochimica Acta, 58, 5147–5159.

Roberts, M.W. (1991) Evidence for the role of surface transients and precursor states in determining molecular pathways in surface reactions. Applied Surface Science, 52, 133–140.

Sandell, E.B. (1944) Colorimetric determination of traces of metals. Inerscience Publishers, New York.

Sasaki, K. (1994) Effect of grinding on the rate of oxidation of pyrite by oxygen in acid solutions. Geochimica et Cosmochimica Acta, 58, 4649–4655.

Sasaki, K., Tsunekawa, M., Ohtsuka, T., and Konno, H. (1995) Confirmation of a sulphur-rich layer on pyrite after oxidative dissolution by Fe^{3+} ions around pH 2. Geochimica et Cosmochimica Acta, 59, 3155–3158.

Schoonen, M.A.A. and Barnes, H.L. (1991) Reactions forming pyrite and marcasite from solution: I. Nucleation of FeS_2 below 100 °C. Geochimica et Cosmochimica Acta, 55, 1495–1504.

Scofield, J.H. (1976) Hartree-Slater subshell photoionization cross-stions at 1254 and 1487 eV. Journal of Electron Spectroscopy and Related Phenomena, 8, 129–138.

Shirley, D.A. (1972) High-resolution X-ray photoemission spectrum of the valence bands of gold. Physics Reviews, 5, 4709–4714.

Singer, P.C. and Stumm, W. (1970) Acid mine drainage: The rate limiting step. Science, 167, 1121–1123.

Smith, E.E., Suanles, K., and Schumate, K. (1968) Sulfide to sulfate reaction studies. In Proceedings of the second symposium on coal mine drainage research, p. 1–11. Bituminous Coal Research Inc., Monroebille, Pennsylvania.

Taylor, B.E., Wheeler, M.C., and Nordstrom, D.K. (1984) Isotope composition of sulphate in acid mine drainage as measure of bacterial oxidation. Nature, 308, 538–541.

Tossel, J.A., Vaughan, D.J., and Burdett, J.K. (1981) Pyrite, marcasite, and arsenopyrite type minerals: Crystal chemical and structural principles. Physics and Chemistry of Minerals, 7, 177–184.

Wiersma, C.L. and Rimstidt, J.D. (1984) Rates of reaction of pyrite and marcasite with ferric iron at pH 2. Geochimica et Cosmochimica Acta, 48, 85–92.

Williamson, M.A. and Rimstidt, J.D. (1994) The kinetics and electrochemical rate-determining step of aqueous pyrite oxidation. Geochimica et Cosmochimica Acta, 58, 5443–5454.

Wollast, R. (1967) Kinetics of the alteration of K-feldspar in buffered solutions at low temperature. Geochimica et Cosmochimica Acta, 31, 635–648.

Manuscript received August 3, 1996
Manuscript accepted June 3, 1997